

Investigating the Impact of Plain Flap as Lift Enhancement on Symmetrical Airfoils

Yohanes Mangatur Parluhutan¹, Fahrudin², Damora Rhakasywi³

(Received: 23 January 2024 / Revised: 15 February 2024 / Accepted: 9 March 2024)

Abstract—Symmetric airfoils like NACA 0015 have limitations in generating lift force compared to asymmetric airfoils. Therefore, additional devices are needed to overcome this limitation, A plain flap is one of a device that can be used to enhance the lift force on the airfoil. This study aims to analyze the impact of a plain flap on the aerodynamic performance of the NACA 0015 airfoil, emphasize the Lift Coefficient (C_l) and Drag Coefficient (C_d). Data for this research is collected through the utilization of Computational Fluid Dynamic method. Simulations were run at a Reynolds number of 4×10^6 using the k-Epsilon turbulent model. Three variations of geometry models were simulated: NACA 0015 base model and NACA 0015 airfoil with a plain flap at a deflection angle of 15° and 30° . All three geometry models were subjected to variations in the Angle of Attack that ranges from 0° to 25° . The results demonstrate that implementing a plain flap at deflection angles of 15° and 30° significantly increases the maximum airfoil's coefficient of lift. The initial maximum lift coefficient of NACA 0015 is 1.15 improved to 1.5 and 1.71, respectively. However, incorporating a plain flap result in a notable rise in drag. On average, the Drag Coefficient experiences a 65% increase at a plain flap angle of deflection of 15° and a 178% increase at a plain flap angle of deflection of 30° .

Keywords—Aerodynamic, NACA 0015, Numerical Simulation

I. INTRODUCTION

Airfoil is a streamlined profile that divides airflow into two parts over and under the wings. The design ensures acceleration of air over the upper surface due to Bernoulli's principle, which states that increased fluid velocity translates to decreased static pressure. This velocity difference creates a pressure discrepancy, resulting in lift force generation [1]. One of the airfoil models is the symmetrical airfoil. Symmetrical airfoils have the advantage of aerodynamic stability but have limitations in generating sufficient lift. To overcome these limitations, an additional device is needed to create additional lift force when necessary. One commonly used device is the plain flap, a flow control device that is positioned passively at trailing edge of airfoil [2]. Research is needed to analyze the extent to which the use of a plain flap on an airfoil can increase lift. Furthermore, the implications of using a plain flap on the drag created also need to be investigated. This research focuses on analyzing one of the symmetric airfoils, NACA 0015, using Computational Fluid Dynamic (CFD) at high speeds with a Reynolds number of 4×10^6 . The study is conducted by varying the Angle of Attack (AoA) between 0° - 25° , as well as the deflection angle of the flap at 15° and 30°

Numerous investigations have been carried out to analyze the effects of using a various type of flaps, including their impact on airfoils performance. One such study was carried out by Abhisek, who investigated the performance of a NACA 4415 airfoil

with the addition of a plain flap. Through this analysis, it was noticed that the deflection angle of the flap had a critical impact in determining whether it would generate lift or act as a source of drag on the airfoil. By examining the results obtained from their analysis, Abhisek delved into the concept of "aerodynamic braking," whereby the introduction of drag on the airfoil affects its overall performance [2]. Another research is conducted by Suyitnadi, his research aimed to test the performance of an NACA 0015 airfoil equipped with a split flap through pure experimentation. The study focused on Finding the drag and lift coefficients values for various flap deflection angles. This research highlights the importance of larger flap deflection angles to enhance the aerodynamic effectiveness of the NACA 0015 airfoil during takeoff and landing phases [3]. Another model of flap is also researched by Ilham Wibowo, aimed to increase the lift coefficient of a symmetric NACA 0015 airfoil by adding a Gurney flap at the leading edge. The Gurney flap was added with variations in height at 2%, 4%, 6%, and 8% of the chord length. The results showed that the highest lift coefficient, at 0.046, was achieved by the airfoil with an 8% chord-length Gurney flap at an AoA of 14° . The lowest drag coefficient, at 0.014, was obtained by the airfoil with a 4% Gurney flap at an angle of attack of 0° [4]. In a study conducted by Julian using CFD approach to analyze bionic flaps effect on the asymmetrical NACA 4415 airfoil. Simulations were conducted at three Reynolds number variations ($Re = 10^6$, $Re = 5 \times 10^5$, and $Re = 3 \times 10^5$) within an AoA range of 0° - 25° . The integration of bionic flaps resulted in improved lift performance at high AoA, while

Yohanes Mangatur Parluhutan, Departement of Mechanical Engineering, Universitas Pembangunan Nasional "Veteran" Jakarta, Jakarta, 12450, Indonesia. E-mail: yohanes.mangaturp@gmail.com
Fahrudin, Departement of Mechanical Engineering, Universitas Pembangunan Nasional "Veteran" Jakarta, Jakarta, 12450, Indonesia. E-mail: fahrudin@upnvj.ac.id

Damora Rhakasywi, Departement of Mechanical Engineering, Universitas Pembangunan Nasional "Veteran" Jakarta, Jakarta, 12450, Indonesia. E-mail: rhakasywi4@gmail.com

causing reduced lift performance at low AoA. The addition of bionic flaps also delayed stall onset. At AoA 10° – 13° , all Reynolds number variations exhibited increased drag coefficient (C_d) performance. The computational tests indicated a negative pitch moment (C_m), resulting in a pitch-down effect due to negative torque performance [5]. Hussein investigated the impact of overlap, gap, and flap chord on the NACA 24012's aerodynamic properties using single slotted flaps at a zero AoA. The study employed Fluent analysis with a Reynolds number of 3.1×10^6 . Results showed that larger flap chords increased the lift coefficient but also caused a drag penalty. Extending the flap by 3% C significantly reduced the attainable lift coefficient. Simulation results suggested an optimal gap size of 1% C for maximum lift capability. The study validated the CFD model against field measurements [6].

II. Method

A. Geometry Model

NACA 0015 is the airfoil model that is investigated in this study. This specific airfoil has no camber and is symmetrical, indicated by the initial two numbers '00'. Additionally, the ratio of thickness to chord length for the NACA 0015 airfoil is 15%, as denoted by the number '15' [7]. In this study, three variations of geometric models will be simulated: NACA 0015's base model and NACA 0015 with a flap angled at 15° and 30° . The chord length in this research is one meter. The plain flap on the airfoil is constructed to be 20% of the total length of the airfoil [2] The specific geometry is visible in Figure 1.

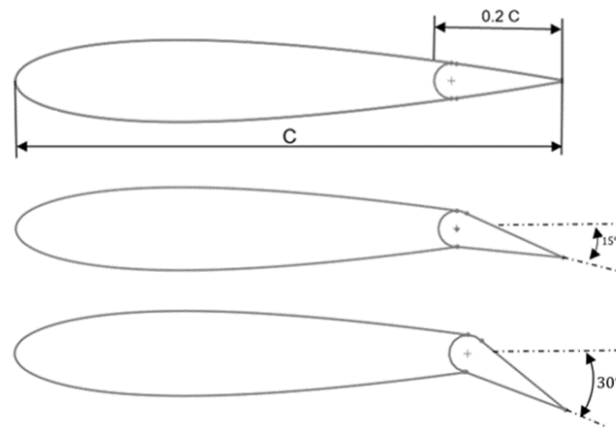


Figure 1. Geometry Model

B. Computation Domain

The computation is performed within a computational domain in the shape of a C surrounding the airfoil. The configuration of the domain includes a combination of a semicircle and a rectangle. The semicircle has a radius of 12.5 times chord length.

Additionally, the rectangular shape has dimensions of 20 times chord length in width and 25 times chord length in height. These dimensions are carefully selected to mitigate any undesirable effects. Figure 2 is an illustration of the domain, while Table 1 presents various computational parameters [8].

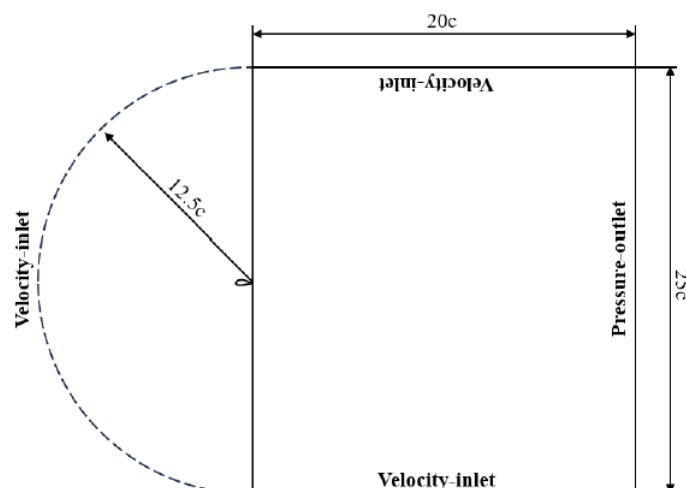


Figure 2. Computation Domain

TABLE 1.
COMPUTATION PARAMETER

Parameter	Definition
Reynolds Number	4×10^6
Angle of Attack	$0^\circ - 25^\circ$
Inlet	Velocity Inlet
Outlet	Pressure Outlet
Airfoil	Wall-no Slip

C. The Governing Formula

The principal formula employed in this investigation is the Reynolds Averaged Navier-Stokes (RANS) formula, it is a modified version of the Navier-Stokes equation specifically adapted for CFD simulations. The RANS equation allows for the separation of mean flow components and fluctuations in the fluid flow, enabling more efficient simulation of turbulent flows within the context of CFD. By using the RANS equation, we can describe and understand the complex behavior of fluid flows, especially in turbulent flows. The mathematical formulation of the RANS equation is expressed in Equation 1 and Equation 2 [9]

$$\begin{aligned} \frac{\partial \rho}{\partial t} + \frac{\partial}{\partial x_i}(\rho u_i) &= 0 \\ \frac{\partial}{\partial t}(\rho u_i) + \frac{\partial}{\partial x_i}(\rho u_i u_j) &= \\ \frac{\partial p}{\partial x_i} + \frac{\partial}{\partial x_j} \left[\mu \left(\frac{\partial u_i}{\partial x_j} + \frac{\partial u_j}{\partial x_i} - \frac{2}{3} \delta_{ij} \frac{\partial u_i}{\partial x_i} \right) \right] & \\ + \frac{\partial}{\partial x_i}(-\rho) \overline{u_i' u_j'} & \end{aligned} \quad (2)$$

III. RESULTS AND DISCUSSION

A. Grid Independent Test

Grid independent test is a crucial step in CFD simulations to evaluate the appropriateness of the mesh element count used. It matters since the quantity of elements may have an impact on the simulation's outcomes. The purpose of this testing is to guarantee that the quantity of elements selected is adequate, ensuring that the outcomes of the simulation remain consistent even with a significant increase in the number of elements. In this research, triangle elements with structured mesh types were utilized.. Mesh independence testing was performed on meshes with 25000, 50000, and 100000 elements. [12]

Obtaining velocity data from a specified reference point is necessary to perform the independence test. [13]. Initially, Equation 5 is used to calculate the mesh element variation ratio that will be employed, followed by the calculation of the order value through Equation 6. The next step involves computing the Grid Convergence Index (GCI) which consists of two components: GCI coarse (Equation 7) indicating the difference in error between the fine and coarse meshes, and the GCI fine (Equation 8) analyzing the difference in fine and medium mesh sizes. Equations 9 and 10 are then used to examine the GCI results in order to ensure

The model that is most frequently chosen among the several turbulent models is the k-ε [10]. The typical k-ε model able to manage a variety of fluid flow situations and is appropriate for simulating both internal and exterior flows. Additionally, this model works well for choosing the basic design, initial iteration, and parameter studies[11]. The formula of k-ε model is expressed in Equation 3 and Equation 4

$$\frac{D}{D_t}(\rho k) = \frac{\partial}{\partial x_j} \left[\left(\mu + \frac{\mu_t}{\sigma_k} \right) \frac{\partial k}{\partial x_j} \right] + G_k - \rho \varepsilon \quad (3)$$

$$\frac{D}{D_t}(\rho \varepsilon) = \frac{\partial}{\partial x_j} \left[\left(\mu + \frac{\mu_t}{\sigma_\varepsilon} \right) \frac{\partial \varepsilon}{\partial x_j} \right] \quad (1)$$

$$+ C_{e1} \frac{\varepsilon}{k} G_k - \rho C_{e2} \frac{\varepsilon^2}{k} \quad (4)$$

that the range of mesh variants chosen is appropriate, aligning with the best mesh category for this study [14]. The values near to 1 in the test results show that the mesh modifications follow the convergence index range. The procedure for figuring out the ideal grid count involves identifying the error value that is the lowest, leading to the utilization of the fine mesh (100000 elements) configuration throughout the computational process. The Grid independent test's overall final outcome is summed up in Table 2.

$$r = \frac{h_2}{h_1} \quad (5)$$

$$\bar{p} = \frac{\ln \left(\frac{f_{fine} - f_{medium}}{f_{medium} - f_{coarse}} \right)}{\ln(r)} \quad (6)$$

$$GCI_{coarse} = \frac{F_s | \varepsilon_{coarse} | r^{\bar{p}}}{(r^{\bar{p}} - 1)} \quad (7)$$

$$GCI_{fine} = \frac{F_s | \varepsilon_{fine} | r^{\bar{p}}}{(r^{\bar{p}} - 1)} \quad (8)$$

$$\frac{GCI_{fine}}{GCI_{coarse} r^{\bar{p}}} \approx 1 \quad (9)$$

$$f_{rh=0} = f_{fine} + \frac{(f_{fine} - f_{medium})}{(r^{\bar{p}} - 1)} \quad (10)$$

TABLE 2.
 GRID INDEPENDENCE TEST RESULTS

Variation	Coarse	Medium	Fine
Velocity	63.5062	63.3673	63.3110
$F_{th}=0$	-	63.27263	-
r	-	2	-
p	-	1.303	-
GCI_{coarse}	-	0.1868%	-
GCI_{fine}	-	0.076%	-
Results	-	1	-
Mesh Errors	0,3692%	0.1496%	0.0606%

B. Data Validation

Validation is carried out to ensure the accuracy of the computational processes and the similarity of the results to real-world conditions. The validation process involves comparing the simulated values of C_l and C_d with experimental data conducted by Kekina at a Reynolds number of 360.000 [15]. The validation results are depicted in Figure 3. The graphs illustrating the variations of C_l and C_d with the AoA exhibit comparable trends, although discrepancies arise after the stall condition due to the challenging nature of predicting airfoil behavior in that regime. Consequently, it can be inferred that the computational results are deemed valid based on the comparison between the two datasets.

C_l , C_d , and the C_l/C_d ratio, which serves as a measure of the aerodynamic efficiency of airfoil. Figure 4 presents a graph of C_l against AoA for each geometrical model. It can be observed that the use of a plain flap significantly increases C_l at 0° AoA. The lift coefficient, which was almost 0 at 0° AoA in NACA 0015 base model, can be increased to 0.84 with a plain flap deflection of 15° and 1.45 with a plain flap deflection of 30° . The optimum value of C_l can also be increased by enhancing the airfoil with a plain flap. In the case of a airfoil without flap, the peak of C_l is 1.15 at an AoA of 15° before stall. After using a plain flap with a deflection of 15° , the maximum C_l increases to 1.5 at an AoA of 13° . The maximum C_l with a flap deflection of 30° is 1.71 at an AoA of 10° . Although there is an increase in the optimum C_l , it needs to be

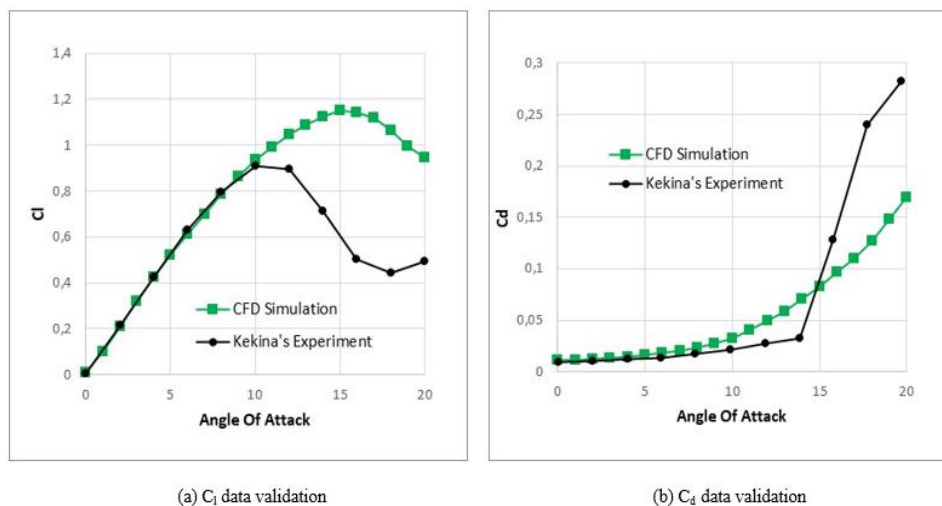


Figure 3. Data Validation

C. Aerodynamic Force Analysis

The data for this research was obtained from CFD simulations at a Reynolds number of 4×10^6 . Three geometrical models were simulated, base model of NACA 0015 and NACA 0015 equipped with plain flaps deflected at 15° and 30° . The analyzed data includes the

compensated for the advancement AoA of the stall [16]. In the normal airfoil condition, stall occurs at an AoA of 15° . With a flap deflection of 15° , stall occurs at 13° , and with a flap deflection of 30° , stall occurs at 10°

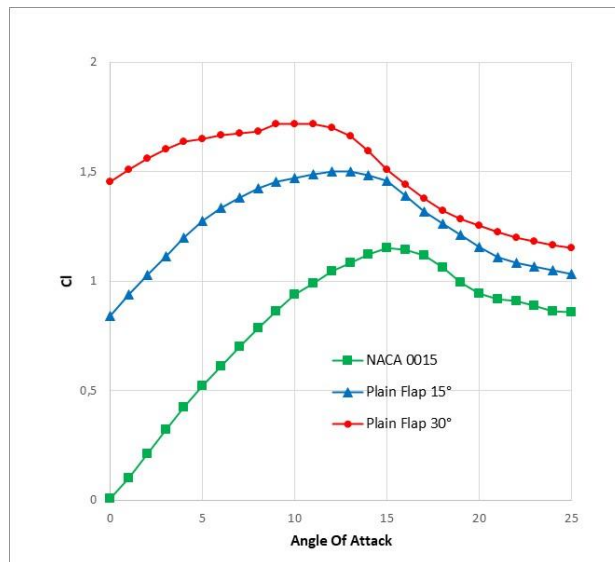


Figure 4. Plot of C_l against AoA

Although the use of a plain flap can increase the lift force on an airfoil, this must be compensated for by a significant increase in drag force[17]. Figure 4 presents a graph of drag coefficient (C_d) against AoA for the three airfoil geometries. It is evident that when the AoA

risks, the C_d increased proportionally in all three airfoil models. The use of a plain flap with a deflection of 15° in average increases the C_d by 65%, while a plain flap with a deflection of 30° results in a significant in average increase of 179% in C_d .

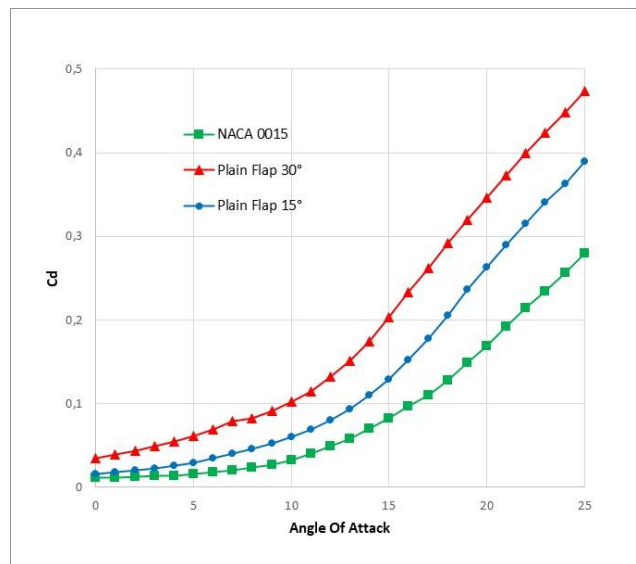


Figure 5. Plot of C_d against AoA

The C_l/C_d ratio is a crucial factor in evaluating the effectiveness of an airfoil's aerodynamics. In the case of NACA 0015 base model, the efficiency value increases proportionally with the increase in AoA within the range of 0°-7°, and then decreases after 7°. The efficiency of the airfoil with a flap decreases as the AoA increases. The use of a flap with a deflection of

15° gives better efficiency compared to a deflection of 30°. Among the three geometrical models, it can be observed in Figure 6 that the airfoil with a plain flap deflected at 15° exhibits the best efficiency within the range of 0°-5° AoA.

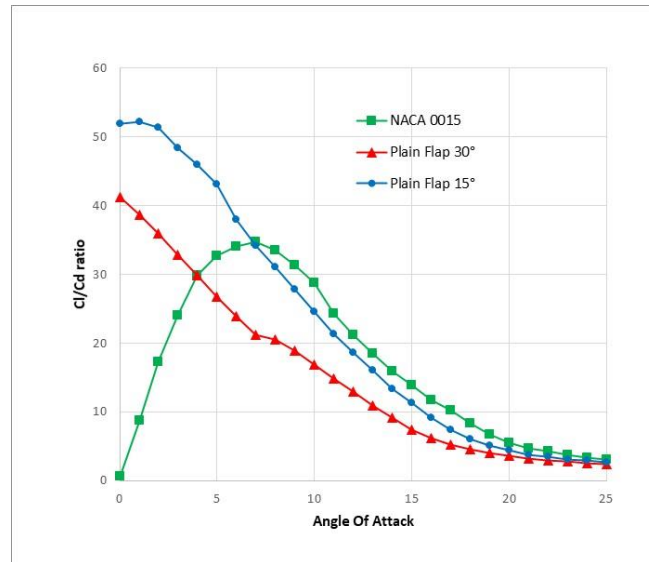
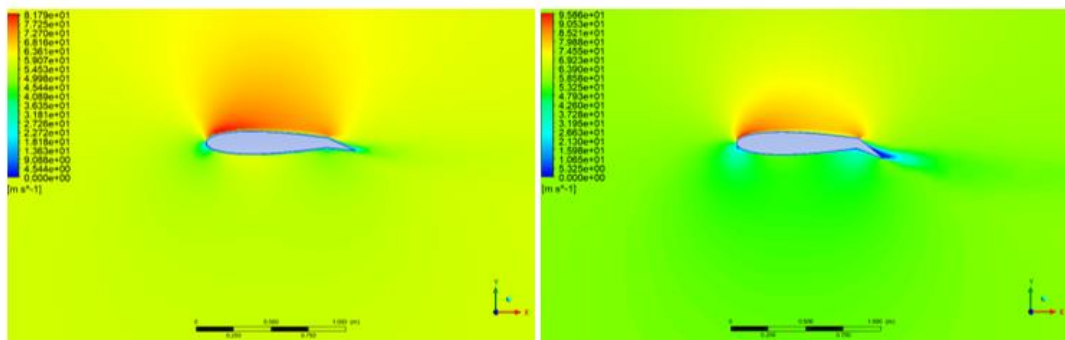


Figure 6. Plot of C_l/C_d ratio against AoA

D. Contour Analysis

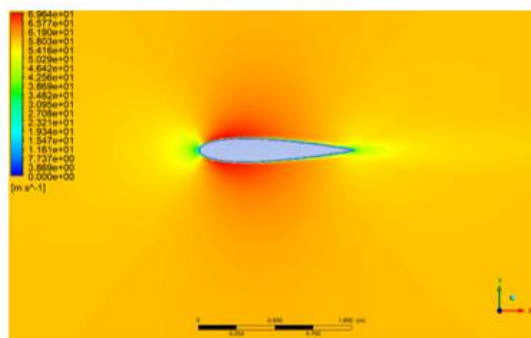
for further analysis, velocity and pressure contour visualization around airfoil was conducted. Figure 7 shows the velocity contour of the NACA 0015 base model and NACA 0015 airfoil equipped with plain flap at deflection angles of 15° and 30°. This analysis was

performed at a Reynolds number of 4×10^6 with a 0° angle of attack. NACA 0015 exhibits symmetric characteristics, as a result, the airfoil's flow on its top and bottom surfaces has almost equal velocities. But once the plain flap is in place, it is clear that the flow is accelerating on the airfoil's upper surface, especially with a deflection angle of 30°.



(a) NACA 0015 with plain flap 15°

(b) NACA 0015 with plain flap 30°



(c) NACA 0015 without plain flap

Figure 7. Velocity Contour

According to Bernoulli's principle, pressure below the airfoil increases as a result of the increased flow rate above the airfoil. The pressure contour in Figure 8 makes this clear. Pressure is applied more to the airfoil's bottom surface than its upper surface. This pressure

disparity creates additional lift force on the airfoil. Therefore, employing a plain flap as a passive flow control mechanism is capable of manipulating the flow around it to generate additional lift.

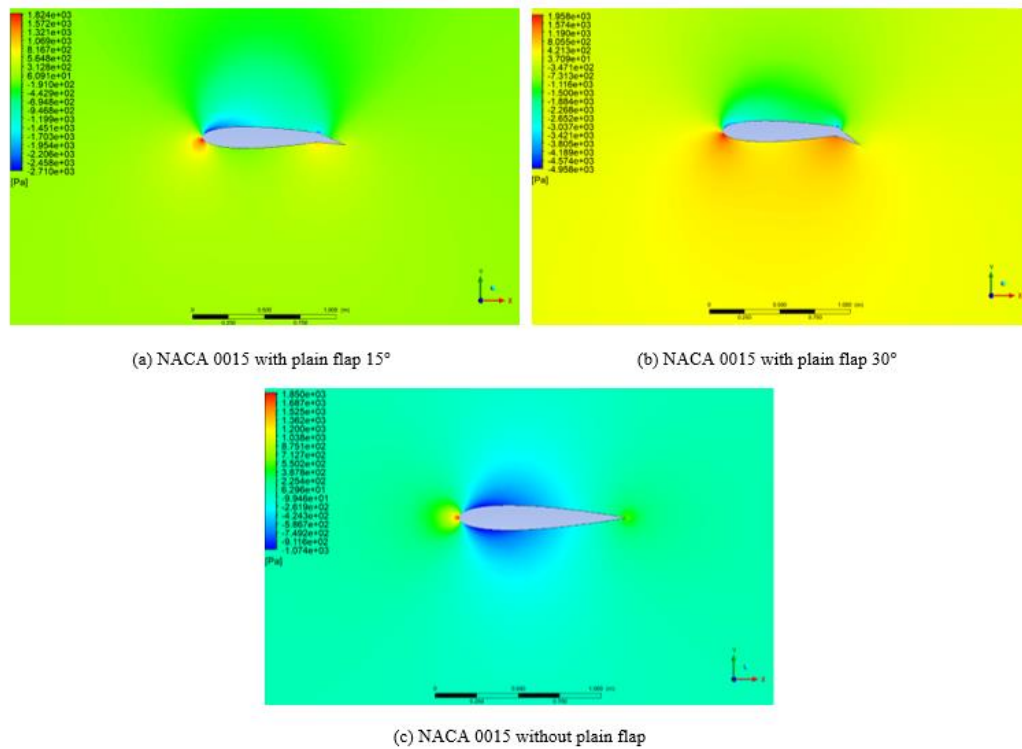


Figure 8. Pressure Contour

IV. CONCLUSION

The purpose of this study is to investigate the impact of plain flap installed on NACA 0015 airfoil. This study aims to analyze the aerodynamic performance, with a focus on lift coefficient and drag coefficient of the airfoil. Data in this study is obtained with Computational Fluid Dynamic method, and the fluid flow simulation on the NACA 0015 airfoil geometry at Reynolds number 4×10^6 shows that the use of a plain flap as a passive device for controlling flow has a significant impact on its aerodynamic performance. At the same Angle of Attack, the use of a plain flap with deflection angles of 15° and 30° can significantly increase the lift coefficient, although it is accompanied by a considerable increase in drag coefficient. The use of a plain flap also causes the stall angle to occur earlier. Without the flap, stall occurs at a AoA 15° . After applying a flap with a deflection angle of 15° , stall occurs at AoA 13° , and with a deflection angle of 30° , stall occurs AoA 10° .

The increase in lift coefficient occurs because the flap accelerates the flow across the airfoil's upper surface, which raises the pressure below the airfoil relative to the flow above it. This pressure difference creates additional lift force on the airfoil. Variations in the fluid's pressure and velocity surrounding the airfoil can be observed from contour analysis. In terms of aerodynamic efficiency, the use of a plain flap with a deflection angle of 15° in the range of AoA 0° - 5° shows the best aerodynamic efficiency. The research findings indicate that incorporating a plain flap on symmetric airfoils like the NACA 0015 airfoil is an effective method for enhancing lift force and able to improve aerodynamic efficiency.

References

- [1] R. Islam Rubel, M. Rokunuzzaman, R. R. I, U. M. K, And I. M. Z, "Comparison Of Aerodynamics Characteristics Of Naca 0015 & Naca 4415 Aerofoil Blade," *Article In International Journal Of Research-Granthaalayah*, Vol. 5, No. 11, P. 187, 2017, Doi: 10.5281/Zenodo.1095406.
- [2] G. Abhishek Vinod And T. J. S. Jothi, "Effect Of Flap Deflection Angle On Flow Characteristics Of Aerofoil," *Iop Conf Ser Mater Sci Eng*, Vol. 1189, No. 1, P. 012039, Oct. 2021, Doi: 10.1088/1757-899x/1189/1/012039.
- [3] Suyitnadi, "Analisis Kinerja Flap Sebagai Penambah Koefisien Gaya Angkat," 2000.
- [4] I. Wibowo, B. Radiant Utomo, D. Gustiani, And M. Iwan, "Pengaruh Penambahan Gurney Flap Pada Airfoil Naca 0015," 2023.
- [5] J. Julian, S. A. Siswanto, F. Wahyuni, D. Nely, And T. Bunga, "Analisis Penggunaan Bio Flap Pada Naca 4415 Dengan Metode Numerik Analisis Of The Use Of Bio Flap On Naca 4415 With Numerical Methods," Vol. 5, Pp. 251–262, 2023.
- [6] E. Q. Hussein, H. Nadhom Azziz, And F. L. Rashid, "Aerodynamic Study Of Slotted Flap For Naca 24012 Airfoil By Dynamic Mesh Techniques And Visualization Flow," Yildiz Technical University Press, 2021.
- [7] R. Islam Rubel, Md. Kamal Uddin, Md. Zahidul Islam, And Md. Rokunuzzaman, "Numerical And Experimental Investigation Of Aerodynamics Characteristics Of Naca 0015 Aerofoil," *International Journal Of Engineering Technologies Ijet*, Vol. 2, No. 4, Pp. 132–141, Apr. 2017, Doi: 10.19072/ijet.280499.
- [8] J. Yao *Et Al.*, "Numerical Simulation Of Aerodynamic Performance For Two Dimensional Wind Turbine Airfoils," In *Procedia Engineering*, 2012, Pp. 80–86. Doi: 10.1016/J.Proeng.2012.01.994.
- [9] S. M. A. Aftab, A. S. M. Rafie, N. A. Razak, And K. A. Ahmad, "Turbulence Model Selection For Low Reynolds Number Flows," *Plos One*, Vol. 11, No. 4, Apr. 2016, Doi: 10.1371/Journal.Pone.0153755.
- [10] Douvi C. Eleni, "Evaluation Of The Turbulence Models For The Simulation Of The Flow Over A National Advisory Committee For Aeronautics (Naca) 0012 Airfoil," *Journal Of Mechanical Engineering Research*, Vol. 4, No. 3, Mar. 2012, Doi: 10.5897/Jmer11.074.
- [11] B. Launder And D. Spalding, "The Numerical Computation Of Turbulent Flows," *Numerical Prediction Of Flow, Heat Transfer, Turbulence And Combustion*, Pp. 96–116, Jan. 1983, Doi: 10.1016/B978-0-08-030937-8.50016-7.

- [12] M. F. Lukiano, J. Julian, F. Wahyuni, And W. Iskandar, "The Influence Of Mounting Angle On Gurney Flap On The Aerodynamics Performance Of Naca 0015 Using Cfd Method," 2023.
- [13] J. Julian, R. A. Anggara, And F. Wahyuni, "Influence Of Slat Size Variation As Passive Flow Control Instruments On Naca 4415 Airfoil Toward Aerodynamic Performance," 2023.
- [14] J. Julian, W. Iskandar, And F. Wahyuni, "Leading Edge Modification Of Naca 0015 And Naca 4415 Inspired By Beluga Whale," 2023.
- [15] P. Kekina And C. Suvanjumrat, "A Comparative Study On Turbulence Models For Simulation Of Flow Past Naca 0015 Airfoil Using Openfoam," In *Matec Web Of Conferences*, Edp Sciences, Feb. 2017. Doi: 10.1051/Mateconf/20179512005.
- [16] S. Obeid, R. Jha, And G. Ahmadi, "Rans Simulations Of Aerodynamic Performance Of Naca 0015 Flapped Airfoil," *Fluids*, Vol. 2, No. 1, Mar. 2017, Doi: 10.3390/Fluids2010002.
- [17] T. Ahmed, M. Tanjin Amin, S. Rafiul Islam, And S. Ahmed, "Computational Study Of Flow Around A Naca 0012 Wingflapped At Different Flap Angles With Varying Mach Numbers," 2013.